*Anal. Chem.* **2010,** *82,* 3581–3587

# Si:$WO_3$ Sensors for Highly Selective Detection of Acetone for Easy Diagnosis of Diabetes by Breath Analysis

**Marco Righettoni, Antonio Tricoli, and Sotiris E. Pratsinis***

*Particle Technology Laboratory, Department of Mechanical and Process Engineering, Institute of Process Engineering, ETH Zurich, CH-8092 Zurich, Switzerland*

**Acetone in the human breath is an important marker for noninvasive diagnosis of diabetes. Here, novel chemoresistive detectors have been developed that allow rapid measurement of ultralow acetone concentrations (down to 20 ppb) with high signal-to-noise ratio in ideal (dry air) and realistic (up to 90% RH) conditions. The detector films consist of (highly sensitive) pure and Si-doped $WO_3$ nanoparticles (10−13 nm in diameter) made in the gas phase and directly deposited onto interdigitated electrodes. Their sensing properties (selectivity, limit of detection, response, and recovery times) have been investigated as a function of operating temperature (325−500 °C), relative humidity (RH), and interfering analyte (ethanol or water vapor) concentration. It was found that Si-doping increases and stabilizes the acetone-selective $\varepsilon$-$WO_3$ phase while increasing its thermal stability and, thus, results in superior sensing performance with an optimum at about 10 mol % Si content. Furthermore, increasing the operation temperature decreased the detector response to water vapor, and above 400 °C, it was (≤0.7) always below the threshold (10.6) for fake diabetes detection in ideal conditions. At this temperature and at 90% RH, healthy humans (≤900 ppb acetone) and diabetes patients (≥1800 ppb) can be clearly distinguished by a remarkable gap (40%) in sensor response. As a result, these solid state detectors may offer a portable and cost-effective alternative to more bulky systems for noninvasive diabetes detection by human breath analysis.**

Noninvasive detection of illnesses by human breath analysis[1−4] is an emerging field of medical diagnostics representing a rapid, economic, and simple alternative to standard blood analysis[5,6] and endoscopy.[7,8] The bulk matrix of the breath is a mixture of nitrogen, oxygen, carbon dioxide, water vapor, and inert gases. The remaining small fraction consists of more than 1000 volatile traces with concentrations ranging from parts per trillion (ppt) to parts per million (ppm)[1,9,10] that are either generated in the body (endogenous) or absorbed as contaminants from the environment (exogenous).[11] Some endogenous compounds, including inorganic gases (e.g., NO, CO) and volatile organic compounds (VOCs, e.g. ethane, pentane, ammonia, acetone, ethanol), can be assigned to specific pathologies and, thus, are utilized as breath markers.[1,3] In particular, acetone is a selective breath marker to type-1 diabetes.[1,12] It is produced by hepatocytes via decarboxylation of excess acetyl-coenzyme A.[4] The acetone concentration in the breath increases from 300 to 900 ppb for healthy humans[13] to more than 1800 ppb for diabetic patients.[14] The detection of this small concentration difference (900 ppb) between healthy and ill people in such a complex gas mixture as the human breath requires a highly sensitive and selective acetone sensor.

Several methods have been utilized to analyze trace compounds in the human breath.[2] The most common is gas chromatography (GC) with flame ionization detection (FID),[15] mass spectrometry (MS),[9] or ion mobility spectrometry (IMS).[16] As water vapor, however, can damage the GC column, pretreatment of the breath is necessary before analysis.[17] Selected ion flow tube mass spectrometry (SIFT-MS)[18,19] has shown great potential in real-time concentration monitoring of several breath markers (e.g., acetone, ethanol, ammonia, and isoprene). A major advantage of the latter is its high selectivity, sufficient sensitivity, and low limit of detection (LOD). However, its high cost and limited portability still hinder its application as standard diagnostic tool.[20]

* Corresponding author. E-mail: sotiris.pratsinis@ptl.mavt.ethz.ch.

(1) Cao, W. Q.; Duan, Y. X. *Clin. Chem.* **2006**, *52*, 800–811.
(2) Cao, W. Q.; Duan, Y. X. *Crit. Rev. Anal. Chem.* **2007**, *37*, 3–13.
(3) Manolis, A. *Clin. Chem.* **1983**, *29*, 5–15.
(4) Miekisch, W.; Schubert, J. K.; Noeldge-Schomburg, G. F. E. *Clin. Chim. Acta* **2004**, *347*, 25–39.
(5) American Diabetes Association, *Diabetes Care* **2003**, *26*, 33−50.
(6) Lebovitz, H. E. *Lancet* **1995**, *345*, 767–772.
(7) Lassen, A. T.; Pedersen, F. M.; Bytzer, P.; de Muckadell, O. B. S. *Lancet* **2000**, *356*, 455–460.
(8) Uemura, N.; Okamoto, S.; Yamamoto, S.; Matsumura, N.; Yamaguchi, S.; Yamakido, M.; Taniyama, K.; Sasaki, N.; Schlemper, R. J. *N. Engl. J. Med.* **2001**, *345*, 784–789.
(9) Mukhopadhyay, R. *Anal. Chem.* **2004**, *76*, 273A–276A.
(10) Phillips, M.; Herrera, J.; Krishnan, S.; Zain, M.; Greenberg, J.; Cataneo, R. N. *J. Chromatogr., B* **1999**, *729*, 75–88.
(11) Pleil, J. D.; Lindstrom, A. B. *Clin. Chem.* **1997**, *43*, 723–730.
(12) Henderson, M. J.; Karger, B. A.; Wrenshall, G. A. *Diabetes* **1952**, *1*, 188–193.
(13) Diskin, A. M.; Spanel, P.; Smith, D. *Physiol. Meas.* **2003**, *24*, 107–119.
(14) Deng, C. H.; Zhang, J.; Yu, X. F.; Zhang, W.; Zhang, X. M. *J. Chromatogr., B* **2004**, *810*, 269–275.
(15) Sanchez, J. M.; Sacks, R. D. *Anal. Chem.* **2003**, *75*, 2231–2236.
(16) Lord, H.; Yu, Y. F.; Segal, A.; Pawliszyn, J. *Anal. Chem.* **2002**, *74*, 5650–5657.
(17) Cheng, W. H.; Lee, W. J. *J. Lab. Clin. Med.* **1999**, *133*, 218–228.
(18) Smith, D.; Spanel, P. *Mass Spectrom. Rev.* **2005**, *24*, 661–700.
(19) Spanel, P.; Smith, D. *Med. Biol. Eng. Comput.* **1996**, *34*, 409–419.
(20) Toda, K.; Li, J.; Dasgupta, P. K. *Anal. Chem.* **2006**, *78*, 7284–7291.

10.1021/ac902695n 
Published on Web 04/12/2010

Recently, chemo-resistive detectors based on semiconductor metal oxide films have been applied to the analysis of several breath markers.[21−24] These simple devices have low fabrication cost,[25] offer high miniaturization potential,[26] sensitivity,[27] and sufficient limit of detection (LOD; ppb concentrations).[25] Among the large number of sensing metal oxides,[25] $WO_3$[28,29] and in particular its $\varepsilon$-phase is promising for selective and quantitative detection of acetone in ppb concentrations.[24] This is attributed to the spontaneous electric dipole moment of the $\varepsilon$-phase that increases the interaction with analytes having high dipole moment (e.g., acetone).[30] Nevertheless, such $WO_3$ detectors have been tested only in ideal conditions (dry air) without accounting for the effect of water vapor which is a major component of the human breath.[31] Furthermore, it is well-known that water vapor interferes with the sensing mechanism of semiconductor metal oxides (e.g., $SnO_2$),[32] decreasing their sensitivity (e.g., to EtOH)[33] and leading to an unreliable response.

Here, pure and Si-doped $WO_3$ nanoparticle films[34] are investigated as chemo-resistive acetone detectors. Doping with Si is used to thermally stabilize the acetone selective $\varepsilon$-$WO_3$ phase at the elevated operating temperatures of metal oxide gas sensors (300−500 °C) as an alternative to doping with potentially toxic Cr.[24] The acetone selectivity of these detectors is tested toward water vapor and ethanol, a common VOC in the human breath.[35] The cross-sensitivity to humidity during acetone detection is quantified up to 90% RH. Finally, optimal detector operating temperatures are identified, and the feasibility of ultra low acetone detection (20 ppb) in realistic conditions (90% RH) by these simple Si-doped $\varepsilon$-$WO_3$ detectors is demonstrated.

## EXPERIMENTAL SECTION

**Detector Fabrication.** A flame spray pyrolysis (FSP) reactor was used in combination with a water-cooled substrate holder[36] for synthesis and direct deposition of pure and Si-doped $WO_3$ nanoparticle films onto $Al_2O_3$ substrates featuring a set of interdigitated Au electrodes and a sensing area of 1 $cm^2$ (Figure 1a). Nanoparticles were prepared as follows: Ammonium (meta)-tungstate hydrate (Aldrich, purity >97%) and hexamethyldisiloxane (HMDSO, Aldrich, purity >99%) were mixed, as dictated by the final Si molar content (0−40 mol %) and diluted in a 1:1 (volume ratio) mixture of diethylene glycol monobutyl ether (Fluka, purity >98.5%) and ethanol (Fluka, purity >99.5%) with a total metal atom (Si and W) concentration of 0.2 M. This solution was supplied at a rate of 5 mL/min through the FSP nozzle and dispersed to a fine spray with 5 L/min oxygen (pressure drop 1.5 bar). That spray was ignited by a supporting ring-shaped premixed methane/oxygen flame ($CH_4$ = 1.25 L/min, $O_2$ = 3.2 L/min). Additional 5 L/min sheath oxygen was supplied from an annulus surrounding that flame. Powder samples were collected with a vacuum pump (Vacuumbrand, RE 16) on a water-cooled glass-fiber filter (GF/D Whatman, 257 mm diameter) placed 50 cm above the burner, downstream of the sensor substrate. The nozzle-substrate (NS) distance was 20 cm. The films were annealed and mechanically stabilized in situ by lowering the substrate holder to NS = 14 cm and impinging a particle-free (no metal precursor), xylene-fed spray flame (12 mL/min) onto the film[27] for 30 s. The supporting flame and sheath oxygen flows were those used during FSP deposition.

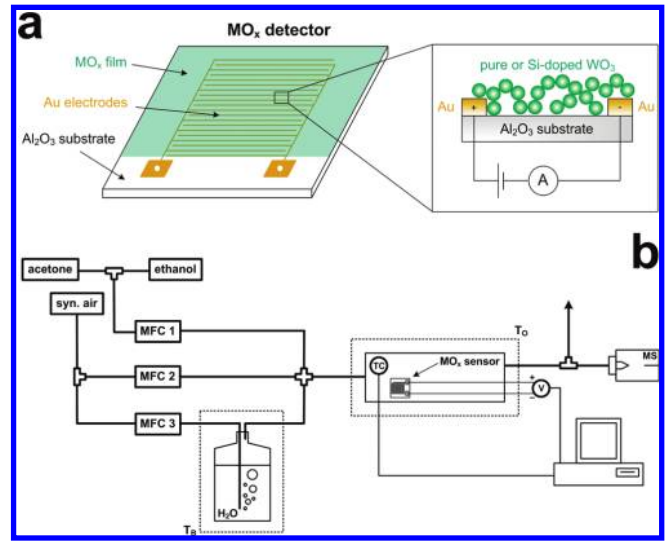


**Figure 1.** (a) Detector schematic: a metal oxide ($MO_x$) film is deposited onto a sensor substrate consisting of an $Al_2O_3$ support with interdigitated Au electrodes. (b) Sensor characterization setup: the acetone and ethanol flows are dosed by mass flow controllers. A humidified air flow from a water bubbler ($T_B$ = 20 °C) is mixed with dry air to obtain the desired relative humidity. The detector is kept in an oven ($T_O$ = 325−500 °C) and connected to a voltmeter to measure the film resistance. The exhaust flow is then analyzed by a mass spectrometer (MS).

**Particle Characterization.** X-ray diffraction patterns were obtained by a Bruker, AXS D8 Advance diffractometer operated at 40 kV, 40 mA at 2$\theta$ (Cu K$\alpha$) = 10−60°, step = 0.04°, and scan speed = 0.8°/min. The crystal size ($d_{XRD}$) was determined using the Rietveld fundamental parameter method with the structural parameters of monoclinic $\gamma$ and $\varepsilon$-$WO_3$.[37,38] The powder specific surface area (SSA) was measured by BET analysis using a Micromeritics Tristar 3000. The BET equivalent diameter was calculated using the density of $WO_3$ (7.16 g/$cm^3$) and $SiO_2$ (2.19


(21) Fleischer, M.; Simon, E.; Rumpel, E.; Ulmer, H.; Harbeck, M.; Wandel, M.; Fietzek, C.; Weimar, U.; Meixner, H. *Sens. Actuators, B: Chem.* **2002**, *83*, 245–249.
(22) Natale, C. D.; Macagnano, A.; Martinelli, E.; Paolesse, R.; D'Arcangelo, G.; Roscioni, C.; Finazzi-Agro, A.; D'Amico, A. *Biosens. Bioelectron.* **2003**, *18*, 1209–1218.
(23) Ryabtsev, S. V.; Shaposhnick, A. V.; Lukin, A. N.; Domashevskaya, E. P. *Sens. Actuators, B: Chem.* **1999**, *59*, 26–29.
(24) Wang, L.; Teleki, A.; Pratsinis, S. E.; Gouma, P. I. *Chem. Mater.* **2008**, *20*, 4794–4796.
(25) Eranna, G.; Joshi, B. C.; Runthala, D. P.; Gupta, R. P. *Crit. Rev. Solid State Mat. Sci.* **2004**, *29*, 111–188.
(26) Graf, M.; Frey, U.; Taschini, S.; Hierlemann, A. *Anal. Chem.* **2006**, *78*, 6801–6808.
(27) Tricoli, A.; Graf, M.; Mayer, F.; Kuhne, S.; Hierlemann, A.; Pratsinis, S. E. *Adv. Mater.* **2008**, *20*, 3005–3010.
(28) Gouma, P. I.; Kalyanasundaram, K. *Appl. Phys. Lett.* **2008**, *93*, 244102.
(29) Khadayate, R. S.; Sali, V.; Patil, P. P. *Talanta* **2007**, *72*, 1077–1081.
(30) Woodward, P. M.; Sleight, A. W.; Vogt, T. *J. Solid State Chem.* **1997**, *131*, 9–17.
(31) Ferrus, L.; Guenard, H.; Vardon, G.; Varene, P. *Respir. Physiol.* **1980**, *39*, 367–381.
(32) Barsan, N.; Weimar, U. *J. Phys.: Condens. Matter* **2003**, *15*, R813–R839.
(33) Tricoli, A.; Righettoni, M.; Pratsinis, S. E. *Nanotechnology* **2009**, *20*, 315502.
(34) Righettoni, M.; Tricoli, A.; Pratsinis, S. E. *Chem. Mater.* **2010**, in press.
(35) Turner, C.; Spanel, P.; Smith, D. *Rapid Commun. Mass Spectrom.* **2006**, *20*, 61–68.
(36) Madler, L.; Roessler, A.; Pratsinis, S. E.; Sahm, T.; Gurlo, A.; Barsan, N.; Weimar, U. *Sens. Actuators, B: Chem.* **2006**, *114*, 283–295.
(37) Salje, E. *Ferroelectrics* **1976**, *12*, 215–217.
(38) Tanisaki, S. *J. Phys. Soc. Jpn.* **1960**, *15*, 573–581.

g/cm$^3$) for the given composition. Transmission electron microscopy (TEM) was conducted with a Hitachi H600, at 100 kV.

**Sensor Characterization.** The morphology and thickness of the deposited sensing films were investigated by scanning electron microscopy (SEM) with a LEO 1530 Gemini (Zeiss/LEO, Oberkochen) and a Tecnai F30 microscope (FEI (Eindhoven); field emission cathode, operated at 2 kV). Prior to sensing tests, the sensors (Figure 1a) were kept in an oven (Carbolite) at 500 °C for 5 h to thermally stabilize them and avoid nanoparticle sintering and, thereby, drift of the sensor signal during testing. The sensor measurements were performed as shown in Figure 1b. Humidified air (MFC 3) was generated by bubbling synthetic air (Pan Gas, 99.999%, and below 0.1 ppm of $C_nH_m$ or $NO_x$) through distilled water maintained at $T_B$ = 20 °C ($p_s$ = 23.38 mbar) to avoid condensation in the pipes. Acetone (10 ppm in synthetic air, Pan Gas 5.0) or ethanol (10 ppm in synthetic air, Pan Gas 5.0) were controlled by a separate mass flow controller (MFC 1) and diluted further with synthetic air (MFC 2) to reach the desired concentration[13,14,35] (from 20 to 3000 ppb). The utilized mass flow controllers ratio (1:500) was well within their maximal ratio (1:10$^5$). The sensors were placed in a quartz tube (3.5 cm in diameter and 35 cm long) located in a tubular furnace (Nabertherm) and connected to a voltmeter (Keithley, 2700 Multimeter/Data acquisition system) to measure the film resistance,[24,39] as it has been done even for breath analysis.[40] The standard total gas flow rate was set to 1 L/min. The operating temperature ($T_O$) was varied between 325 and 500 °C and measured with a n-type thermocouple placed above the sensor. The stream exiting the furnace was analyzed by a mass spectrometer (MS, Pfeiffer, Vacuum Thermostar) at high analyte concentrations (>ppm). Other setups such as in situ heated sensors will give a different but quantitatively consistent sensor response.[27] The sensor response ($S$) is

$$S = R_{air}/R_{analyte} - 1 \quad (1)$$

where $R_{air}$ is the film resistance in air with a given RH and $R_{analyte}$ is the film resistance with a given concentration of acetone or ethanol at the same RH. The sensor response was fairly reproducible between 100 and 600 ppb acetone with a maximum variation of ±9%. The cross-sensitivity to humidity (CS) is

$$CS = abs[(S_{dry} - S_{RH})/S_{dry}]\cdot 100 \quad (2)$$

where $S_{dry}$ and $S_{RH}$ are the responses at dry and a given RH as defined[33] in eq 1. The sensor response time is the time needed to reach 90% of the sensor response to 100 ppb acetone. The recovery time is the time to recover 90% of the sensor response to 600 ppb acetone.

## RESULTS AND DISCUSSION

**Detector Composition.** The gas detectors (Figure 1a) consisted of chemo-resistive pure (Figure 2a) or Si-doped (Figure 2b) $WO_3$ nanoparticle films deposited on sensor substrates.

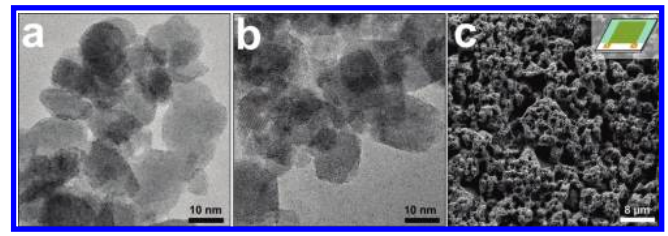


**Figure 2.** TEM images of flame-made (a) pure and (b) 10 mol % Si-doped $WO_3$ nanoparticles collected downstream of the sensor substrate. (c) SEM image of a pure $WO_3$ film directly deposited onto the sensor substrate after in situ annealing.

These films had high porosity (Figure 2c), allowing rapid penetration of the analyte and removal of the sensing reaction products. Pure $WO_3$ particles had a SSA of 64 m$^2$/g, corresponding to an average grain size ($d_{BET}$) of 13 nm, which is sufficiently small to ensure electron depletion of the complete grain (the Debye length of $WO_3$ at 320 °C is 60 nm).[41] The Si-doped particles were similar to pure $WO_3$ ones but were slightly smaller, $d_{BET}$ = 12 and 10 nm for 10 and 20% Si-content, respectively. In fact, Si-doping decreases the sintering rate of metal oxides[42,43] and stabilizes them at the elevated operating temperatures (e.g., 320−500 °C) of sensors resulting in higher gas sensitivity.[44] Furthermore, here, Si-doping from 0 to 20% increased the content of the acetone-selective $\varepsilon$-$WO_3$ phase from 72 to 100 wt % and stabilized 87 wt % of it up to 500 °C (for 5 h in air)[34] resulting in high acetone selectivity, while previous studies on sol−gel made $SiO_2$−$WO_3$ nanoparticles had resulted in only pure $\gamma$-$WO_3$.[39] In comparison, pure $WO_3$ nanoparticles had only 26 wt % $\varepsilon$-$WO_3$ after sintering at 500 °C.

**Acetone Detection in Dry Air.** After injection of the analyte (e.g., acetone, ethanol, or water vapor), the sensor resistance is decreased. This is consistent with the sensing mechanism of n-type semiconductors, such as $WO_3$, to reducing analytes or water vapor.[32] In a simplified description, the resistance of $WO_3$ nanoparticles (and thereby of the sensor) is controlled by the concentration of ionosorbed oxygen species ($O_2^-$, $O^-$, and $O^{2-}$) that trap electrons and act as scattering centers effectively reducing the semiconductor conductivity.[29,45] The acetone reacts with the ionosorbed oxygen ions reducing their concentration and thereby increasing the semiconductor conductivity.[45,46] However, also the reaction with the lattice oxygen should be considered. Two main paths have been proposed for the reaction between acetone and the adsorbed or bulk oxygen:[29]

$$CH_3COCH_{3(gas)} + O_{(adsorbed)}^- \rightarrow CH_3\overset{+}{C}OCH_2 + OH^- + e^- \quad (3)$$

$$CH_3COCH_{3(gas)} + O_{(bulk)} + OH^- \rightarrow CH_3COOH + O_{(vacancies)} + CH_3O^- \quad (4)$$

or

(39) Wang, X. S.; Sakai, G.; Shimanoe, K.; Miura, N.; Yamazoe, N. *Sens. Actuators, B: Chem.* **1997**, *45*, 141–146.
(40) Peng, G.; Tisch, U.; Adams, O.; Hakim, M.; Shehada, N.; Broza, Y. Y.; Billan, S.; Abdah-Bortnyak, R.; Kuten, A.; Haick, H. *Nature Nanotechnol.* **2009**, *4*, 669–673.
(41) Labidi, A.; Lambert-Mauriat, C.; Jacolin, C.; Bendahan, M.; Maaref, M.; Aguir, K. *Sens. Actuators, B: Chem.* **2006**, *119*, 374–379.
(42) Akhtar, M. K.; Pratsinis, S. E.; Mastrangelo, S. V. R. *J. Am. Ceram. Soc.* **1992**, *75*, 3408–3416.
(43) Wu, N. L.; Wang, S. Y.; Rusakova, I. A. *Science* **1999**, *285*, 1375–1377.
(44) Tricoli, A.; Graf, M.; Pratsinis, S. E. *Adv. Funct. Mater.* **2008**, *18*, 1969–1976.
(45) Sahay, P. P. *J. Mater. Sci.* **2005**, *40*, 4383–4385.

$$CH_3COCH_{3(gas)} + O_{(adsorbed)}^- \rightarrow CH_3\overset{+}{C}O + CH_3O^- + e^- \quad (5)$$

$$CH_3\overset{+}{C}O \rightarrow \overset{+}{C}H_3 + CO \quad (6)$$

$$CO + O^- \rightarrow CO_2 + e^- \quad (7)$$

The sensor operating temperature influences the sensing performance both in terms of catalytic activity of the $WO_3$ surface (e.g., reduction reactions)[47−49] and electrical properties of the semiconductor (e.g., activation of defects).[48] Increasing the operating temperature from 320 to 500 °C reduced the pure $WO_3$ film resistance (baseline) in dry air from 2.2 to 0.3 MΩ. These low baselines (<100 MΩ) are required for integration in monolithic gas sensor systems.[50] Increasing the Si-content from 0 to 40% increased the sensor baseline at 320 °C from 2.2 to 142 MΩ, most probably by formation of dielectric $SiO_2$ domains.[44] Nevertheless, the baseline of the Si-doped sensors was decreased to convenient values by increasing the sensor $T_O$ to 400 and 500 °C.

The response of the pure $WO_3$ sensor decreased with increasing $T_O$ from 320 to 500 °C. At 400 °C, it is comparable to that obtained by similar FSP-made $WO_3$ particles deposited by drop-coating,[24] validating the present experimental procedure. The reduction of sensor response with increasing temperature is attributed to the faster reaction kinetics and, thereby, combustion of acetone in the upper layers of the $WO_3$ film that reduces the amount of analyte reaching its bottom.[51] Furthermore, at high temperatures (e.g., 500 °C), that response is decreased also by the insufficient concentration of adsorbed oxygen ions that can react with acetone vapor.[29] A similar behavior is observed for the Si-doped sensors; for the 10 mol % Si, however, the response starts dropping at 500 °C. This could be attributed to the reduced catalytic activity of $SiO_2$-coated surfaces.

Here, the acetone selectivity of the 10% Si-content $WO_3$ sensor is examined in detail, as it had the highest acetone response and relatively low resistance at all temperatures.[34] As discussed above, there are hundreds of gases in the human breath,[1] so detector selectivity is essential in avoiding fake detection of illnesses. Among breath constituents, the ethanol vapor concentration undergoes strong daily variation. The mean ethanol level of a sober human breath is 196 ppb with a standard deviation of 224 ppb.[35] Figure 3 shows the 10% Si-content $WO_3$ sensor response to 100−600 ppb acetone (circles) and ethanol (triangles) in dry air at 400 °C. The sensor response to acetone is 4.7 to 6.7 times higher than that to ethanol whose response was never above 1. This high acetone selectivity against ethanol is comparable to that of Cr-doped ε-$WO_3$ nanoparticles at dry

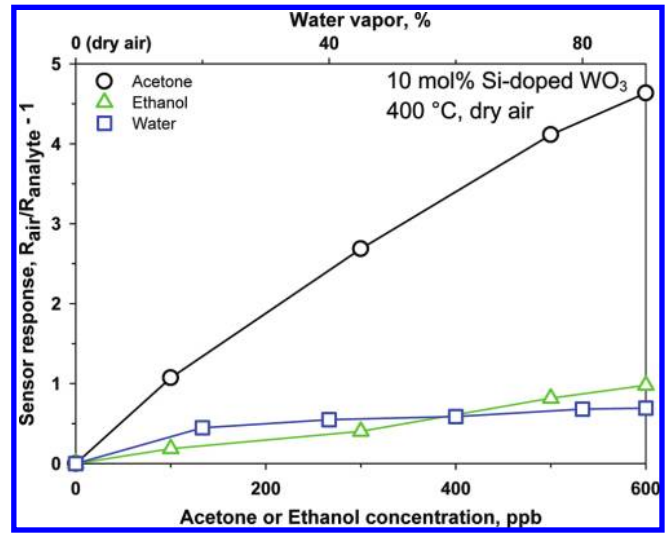


**Figure 3.** Sensor response to acetone (circles), water (squares), and ethanol (triangles) vapors. The sensitivity to acetone is much higher than that to ethanol and water vapors.

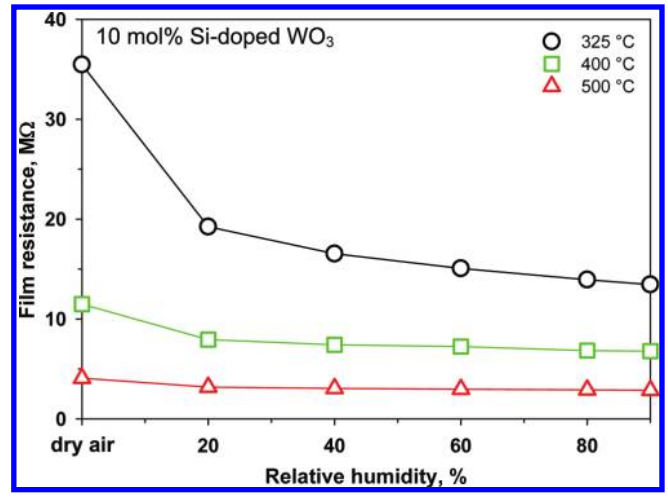


**Figure 4.** Film baselines as function of RH and operating temperature ($T_O$). The effect of the RH is decreased with increasing $T_O$.

conditions.[24] In comparison, the sensor response of the pure $WO_3$ sensor to 600 ppb acetone in dry air at 400 °C was only 1.7 times higher than that to 600 ppb ethanol (not shown here).

Another important component of the human breath is water vapor. The breath relative humidity (RH) varies between 89 and 97% (corresponding to $2.1-2.3 \times 10^7$ ppb).[31] In contrast, the ambient RH usually varies between 20 and 60%. The sudden increase in water vapor concentration during breath sampling could lead to fake acetone detection. To characterize the sensor response to water vapor (Figure 3, squares), the $H_2O$ concentration was increased from dry air to 20, 40, 60, and 90% corresponding to 0.47, 0.94, 1.4, and $2.1 \times 10^7$ ppb. The response to water vapor increased from 0.45 to 0.69 with increasing RH from 20 to 90% and, therefore, was always well below that of 100 ppb acetone.

**Cross-Sensitivity to Relative Humidity.** In general, the response of a metal oxide chemo-resistive gas detector (e.g., $SnO_2$) to an analyte depends also on the relative humidity (RH).[32,33] The % of response change as function of RH % is defined as its cross-sensitivity, CS (eq 2). Characterization of CS is needed as RH can vary during sampling and between

(46) Mitra, P.; Chatterjee, A. P.; Maiti, H. S. *Mater. Lett.* **1998**, *35*, 33–38.
(47) Bendahan, M.; Boulmani, R.; Seguin, J. L.; Aguir, K. *Sens. Actuators, B: Chem.* **2004**, *100*, 320–324.
(48) Aguir, K.; Lemire, C.; Lollman, D. B. B. *Sens. Actuators, B: Chem.* **2002**, *84*, 1–5.
(49) Lee, A. P.; Reedy, B. J. *Sens. Actuators, B: Chem.* **1999**, *60*, 35–42.
(50) Graf, M.; Barrettino, D.; Taschini, S.; Hagleitner, C.; Hierlemann, A.; Baltes, H. *Anal. Chem.* **2004**, *76*, 4437–4445.
(51) Becker, T.; Ahlers, S.; Bosch-v.Braunmuhl, C.; Muller, G.; Kiesewetter, O. *Sens. Actuators, B: Chem.* **2001**, *77*, 55–61.

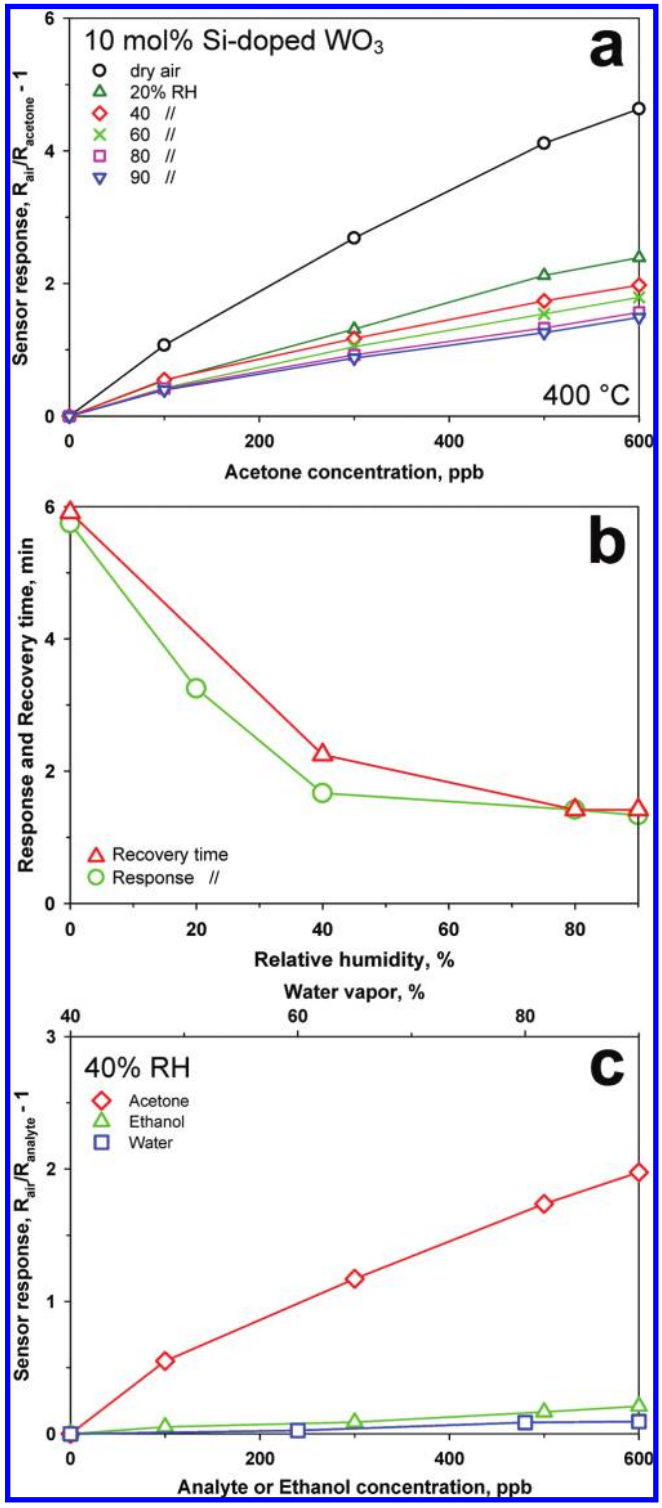


**Figure 5.** (a) Sensor response of a 10 mol % Si-content $WO_3$ sensor at 400 °C upon exposure to increasing acetone concentration at various relative humidities (RH). The sensor response to acetone decreased with increasing RH showing high cross sensitivity (CS = 67%) between 0 and 90% RH. Between 80 and 90% RH, however, the CS was only 4%, showing the robustness of such sensors at the typical RH of the human breath. (b) Response to 100 ppb (circles) and recovery times to 600 ppb (triangles) as a function of RH at 400 °C. Increasing RH reduced both response and recovery times. (c) Sensor signal for different analytes, e.g., acetone (diamonds), ethanol (triangles) at 40% RH, and water (squares). Although, the sensor response to acetone is decreased, its selectivity against ethanol and water vapor is increased over that in dry air (Figure 3).

different breath samples.[31] Figure 4 shows the 10 mol % Si-content sensor baseline as a function of RH at several operating temperatures. At 325 °C (Figure 4, circles), the film resistance decreases steeply from 35.5 to 19.2 MΩ with increasing RH from dry air to 20% and decreases further at 90% RH reaching 13.5 MΩ. Increasing the operating temperature to 400 °C (squares) and 500 °C (triangles) decreases the effect of RH on the sensor baseline. In more detail, at 500 °C, the baseline is reduced from 4 to 2.9 MΩ with increasing RH from dry air to 90%. This is attributed to the reduction of water-related species (e.g., OH) adsorption with increasing temperature. In fact, adsorption of water-related species on metal oxide surfaces increases conductivity[32] at the expense of sensitivity.[33] A similar trend was observed for the pure and 20 mol % Si-content $WO_3$ films. Although the minimal CS to RH is reached at 500 °C, the sensor response to acetone is decreased at this temperature. Furthermore, temperatures below 500 °C are favorable for integration in micro gas sensor systems[50] and to reduce power consumption. These relatively high resistances can be reduced also by interspersing noble metal or CuO nanoparticles serving as nanoelectrodes.[52]

Figure 5a shows the 10 mol % Si-content sensor response to acetone as a function of RH at 400 °C. Increasing the RH from 0 to 90% reduced the sensor response to 600 ppb acetone from 4.6 to 1.5, corresponding to a CS of 67%. This is in agreement with the reduction of sensor response with increasing RH observed by other metal oxides (e.g., $SnO_2$).[33] As a result, simultaneous measurement of RH is necessary to reliably determine acetone concentration. Nevertheless, the highest sensor response reduction is measured between dry air and 20% RH even though dry air is not a realistic condition for breath analysis.[31] As discussed above, the RH of the human breath[31] is around 90%. Here, the CS was only 4% when increasing the RH from 80% (Figure 5a, squares) to 90% (down triangles). This indicates that sufficiently precise detection of acetone in the human breath is possible without additional RH measurement with these Si-doped $WO_3$ sensors. It is remarkable to notice that acetone can be detected up to 90% RH, without the need of any pretreatment of the gas mixture.[17]

Increasing the RH from dry air to 90% decreased the response time from 5.7 to 1.3 min (Figure 5b, circles) and the recovery time from 5.9 to 1.4 min (Figure 5b, triangles) at 400 °C. This can be attributed to the adsorption of water-related species. As at 40% RH several adsorption sites are occupied already (Figure 4), the reaction with acetone does not lead to further adsorption of water-related species, and so, mostly rapid[53] oxygen adsorption/desorption takes place. Figure 5c shows the response of the 10% Si-content sensor to acetone (diamonds), ethanol (triangles), and water vapor (squares) at 400 °C with 40% RH. Although the response to acetone is decreased over that seen in dry air (Figure 3), the selectivity over ethanol and water vapor is increased clearly.

Figure 6 summarizes the effect of Si-content on the sensing properties at 600 ppb of acetone. A similar reduction of the acetone response was observed for all films with increasing RH. Doping

(52) Tricoli, A.; Pratsinis, S. E. *Nature Nanotechnol.* **2010**, *5*, 54–60.
(53) Wahlstrom, E.; Vestergaard, E. K.; Schaub, R.; Ronnau, A.; Vestergaard, M.; Laegsgaard, E.; Stensgaard, I.; Besenbacher, F. *Science* **2004**, *303*, 511–513.

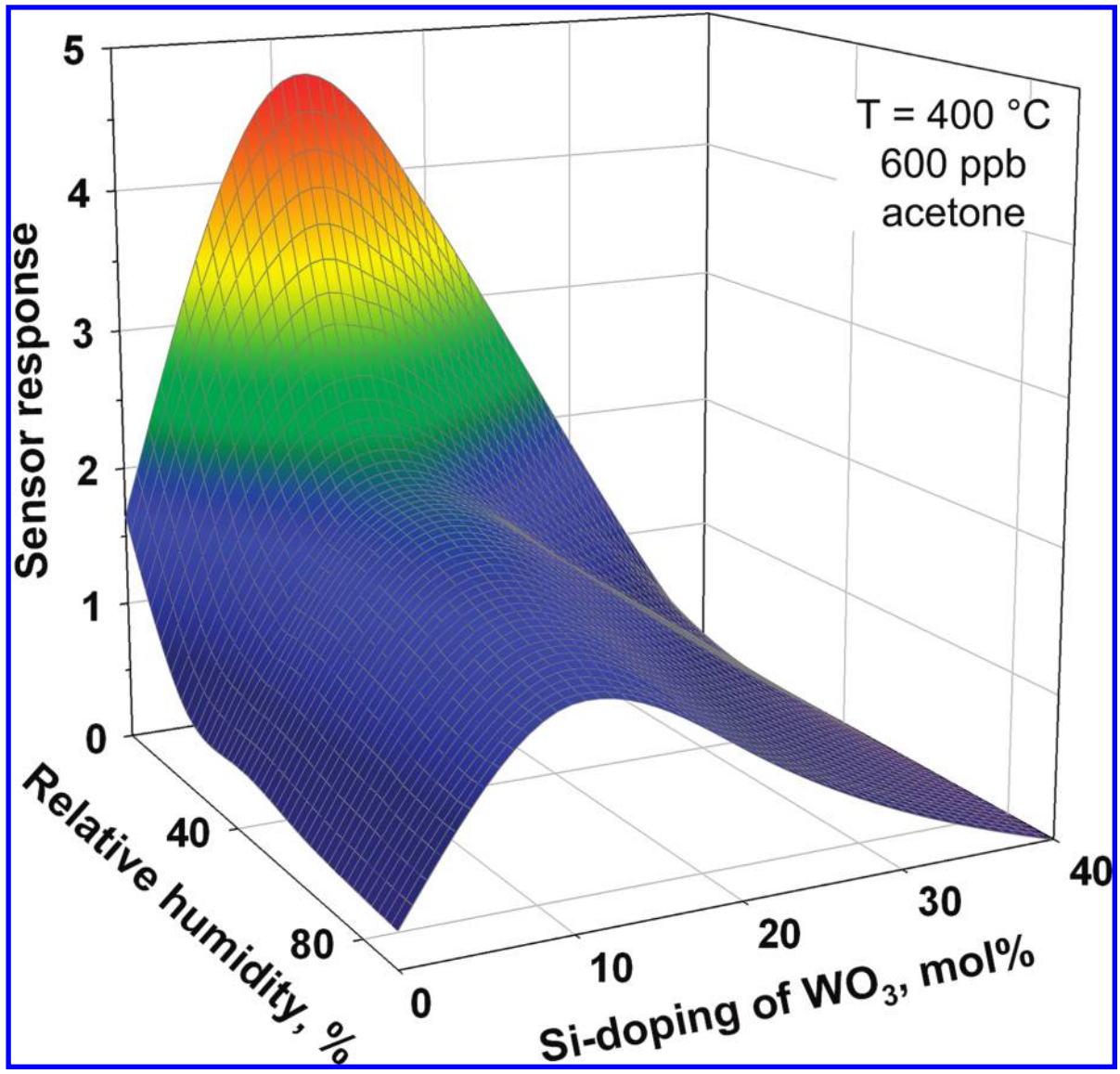


**Figure 6.** $WO_3$-based sensor response to 600 ppb acetone at different relative humidity as a function of Si-content (400 °C). Doping the sensor with 10 mol % Si exhibits an optimal sensor response that is attributed to the higher thermal stability of these nanocomposites. However, increasing further the Si-doping to 40 mol % reduced the sensitivity to acetone to zero, most probably by formation of dielectric $SiO_2$ domains between the $WO_3$ ones.[44] The RH decreased the acetone sensitivity for all sensors, but this effect levels off above 40% RH. Close to 90%, the sensitivity variation as a function of the RH is minimal, indicating the minimal cross-sensitivity of these sensors to RH for breath analysis.

the $WO_3$ sensor with 10 mol % Si exhibits an optimal sensor response that is attributed to the $\varepsilon$-$WO_3$ phase promotion and increased thermal stability[34] by the Si presence. However, increasing further the Si-doping increased the resistance, and at 40 mol % Si, the films had no sensitivity to acetone. A similar behavior was observed during ethanol sensing by Si-doped $SnO_2$ particles insulated eventually by dielectric $SiO_2$ domains.[44]

Figure 7 shows the resistance of a 10% Si-content sensor at 400 °C and realistic RH (90%). After injection of 20 ppb acetone, the resistance was decreased (95 s) from 6.8 to 6.2 MΩ, corresponding to a response of 0.1. This extremely lower limit of detection (LOD) is comparable to that obtained by more complex systems as SIFT-MS.[18] Furthermore, after flushing with humid air, the baseline is rapidly (80 s) recovered. The high signal-to-noise ratio (between 12 and 60) allows precise detection of this extremely low acetone concentration with a relatively simple solid state detector that could be rapidly integrated in portable micro gas sensor systems.[27] Furthermore, the 10% Si-content sensor response to acetone (Figure 8) was below 2 for healthy humans (<0.9 ppm)[13] and above 3.25 for diabetics (>1.8 ppm).[14] This 40% increase in sensor response even at this high RH may allow reliable diagnosis of diabetic patients by breath acetone monitoring with a portable metal oxide detector.

## CONCLUSIONS

Pure and Si-doped $WO_3$ chemo-resistive detectors were utilized for quantitative analysis of acetone concentration, an important breath marker, in ideal (dry air) and realistic (90% RH) conditions. The acetone sensor response (e.g., 4.63 at 600 ppb) at 400 °C in dry air was compared to that of water vapor (e.g., 0.7 at 90% RH) and ethanol (e.g., 0.97 at 600 ppb), demonstrating high acetone selectivity for application in medi-

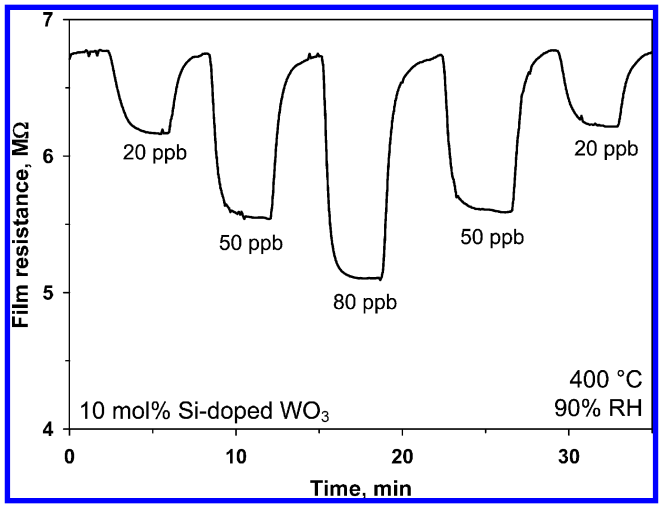


**Figure 7.** $WO_3$ sensor resistance (10 mol % Si-doping) at 90% RH and upon exposure to different ultra low concentrations of acetone (20, 50, and 80 ppb) at 400 °C.

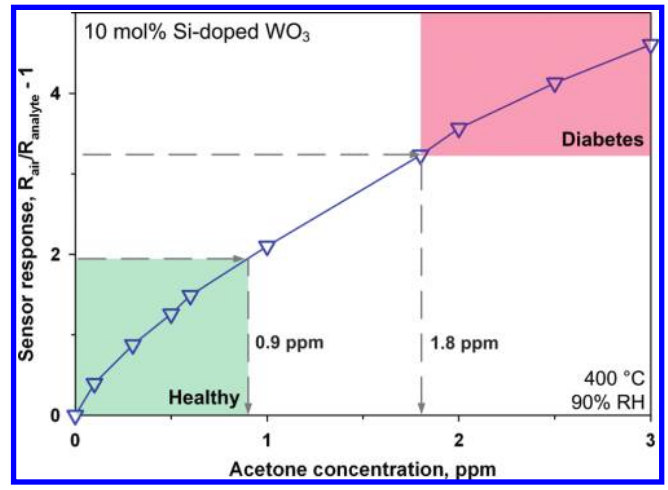


**Figure 8.** Sensor response for acetone detection (0−3 ppm) of a 10 mol % Si-doped $WO_3$ sensor with 90% RH at 400 °C. Diabetic patients (≥1.8 ppm) can be clearly distinguished from healthy humans (≤0.9 ppm) by, at least, 40% difference in sensor response.

cal diagnostics. The sensor responses were maximal below 500 °C while the influence of water vapor was decreased continuously with increasing operating temperature. However, already at 400 °C, the detector baselines were quite stable (e.g., response of 0.7 to 90% RH) against sudden increases in water vapor concentration.

Increasing RH to 90% decreased the response of the 10% Si-content $WO_3$ sensor to 68% of that at 600 ppb in dry air, indicating high cross-sensitivity to relative humidity. Nevertheless, this effect was more pronounced starting from the ideal condition (dry air). In fact, small variations (e.g., 10%) of water vapor content around 90% RH had only minimal effect on the sensor response (e.g., 4%). Although the sensor response to acetone was decreased with increasing RH, the sensor selectivity to acetone was increased. Finally, rapid detection of 20 ppb acetone at such realistic RH conditions was demonstrated by these low cost, solid state devices, showing a great potential for their application in noninvasive diagnosis of diabetes.

## ACKNOWLEDGMENT

We cheerfully acknowledge stimulating discussions with Prof. P. Gouma (Stony Brook University, New York) and thank Dr. F. Krumeich (EMEZ, ETHZ) for the microscopic analysis. This research was supported in part by the CCMX, Nancer, European Space Agency and the Swiss National Science Foundation, grant 200021_130582/1.

Received for review November 25, 2009. Accepted March 22, 2010.

AC902695N